

Undrained monotonic behaviour of pumice sand

R P Orense

Department of Civil and Environmental Engineering, University of Auckland
r.orense@auckland.ac.nz (Corresponding author)

Keywords: pumice sand, undrained test, monotonic behaviour, triaxial test, relative density

ABSTRACT

Because of their lightweight, highly crushable and compressible nature, pumiceous sands are problematic from engineering and construction viewpoint. There has been very little information on their liquefaction characteristics and most empirical procedures available in evaluating the liquefaction potential of sands are derived primarily from hard-grained sands. To understand the liquefaction characteristics of pumice sands, several series of monotonic undrained triaxial tests were conducted on commercially-available pumice sands. Results indicated that specimens reconstituted under loose and dense states practically showed similar response, confirming the earlier findings that relative density did not have significant effect on the behaviour of pumice. The stress-strain relations showed a stiffer response at small strain level, followed by development of large strains and greater dilatancy when the phase transformation state (i.e., from contractive to dilative) was reached. Pumice sands have angle of internal friction at failure of about 42-44°, which is much greater than those of natural hard-grained sands. Even under large strain level, they did not reach steady state of deformation, possibly due to continuous breakage of particles during shearing, which resulted in more resistant soil structure that did not allow deformation at constant shear stress to occur.

1 INTRODUCTION

The active geological past of New Zealand has led to widespread deposits of volcanic soils throughout the country. The Taupo Volcanic Zone (TVZ) in the central region of the North Island in particular has extensive deposits of pumice sands. Pumice is characterised by a number of distinctive properties, such as it is generally lightweight, highly frictional and the coarser particles are also highly degradable and compressible due to their vesicular nature.

To understand better the engineering characteristics of pumice, the author and his colleagues in the Geomechanics group at the University of Auckland have performed a number of laboratory studies (e.g., Pender, 2006; Pender et al., 2006; Kikkawa, 2008; Kikkawa et al., 2009, 2011, 2012; Orense et al. 2012). Some of the tests performed include K_0 compression testing on dry pumice sand with measurement of gas permeability to track particle crushing effects on void space reduction, effect of vertical stress relaxation on the stress-strain relations of dense and loose pumice specimens, as well cyclic undrained triaxial tests.

This paper deals with the monotonic undrained shear behaviour of pumice sand. The undrained behaviour of sandy soils under monotonic shearing is conventionally used to investigate liquefaction mechanism. Monotonic shearing means the specimen in the triaxial cell, which is isotropically consolidated, is subjected to an increasing axial load until failure occurs. During shearing, the drainage valve is closed; this results in generation of excess pore water pressure.

2 SOILS SAMPLES USED AND TESTING METHODOLOGY

The tests were performed on commercially-available pumice sand. This is not a natural deposit but was derived by processing sand from the Waikato River. The particles were centrifugally

separated from the other river sand particles so that the samples consist essentially of pumice grains. Pumice sands with two different grading curves were used: Pumice-A sand (0.075 – 2.5 mm), and Pumice-B sand (0.15 – 0.60 mm). The grain size distribution curves are shown in Figure 1, together with the properties obtained using methods based on NZ Standards (1986).

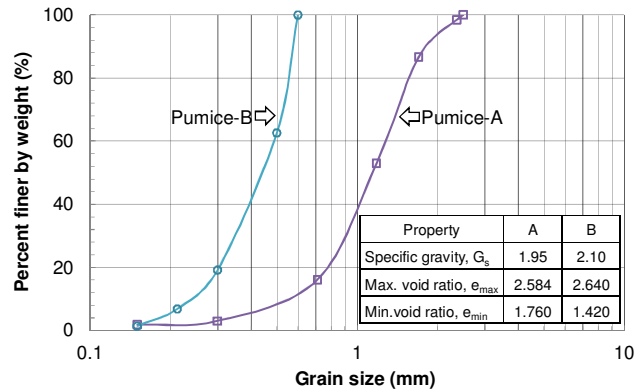


Figure 1. Grain size distribution curves and index properties of soils used.

Because of the presence of voids on the surface and on the particle interior, it was not easy to completely saturate the pumice sand. For this purpose, saturated specimens were made using de-aired pumice sands, i.e., sands were first boiled in water to remove the entrapped air. To prepare the test specimens, the “boiled” sand was water-pluviated into a two-part split mould which was then gently tapped until the target relative density was achieved. Next, the specimens were saturated with appropriate back pressure and then isotropically consolidated at the target effective confining pressure, σ'_c . B-values > 0.95 were obtained for all specimens. The test specimens were 38 mm in diameter and 76 mm high.

The undrained monotonic tests were performed using the gear-type triaxial apparatus. Undrained monotonic loading was applied to the specimens using axial compression. The loading rate for the tests was 0.015 mm/min. To begin shearing, the back pressure valve was closed (undrained test). The target strain was 30% to observe the specimen under the steady state of deformation. Some specimens did not reach this strain level due to a number of factors, such as irregular specimen deformations and erratic load cell readings, rendering the data unreliable.

3 TEST RESULTS AND DISCUSSION

The results of the monotonic undrained tests on reconstituted pumice sands are expressed in terms of the effective stress path (deviator stress vs. mean effective stress) and deviator stress-axial strain relation. Taking σ'_1 and σ'_3 as the maximum and minimum effective principal stresses the triaxial specimen is subjected to, then the deviator stress, $q = \sigma'_1 - \sigma'_3$ and the mean effective stress: $p' = (\sigma'_1 + 2\sigma'_3)/3$. The axial strain is denoted as ϵ_a .

3.1 Effect of Density and Confining Pressure

It is well known that changes in density and confining pressure affect the undrained response of natural sand. The effects were therefore investigated for the pumice sand A by examining the respective deviator stress-axial strain curves and stress paths under different conditions. The pumice samples were reconstituted as triaxial specimen at three different states: loose ($e=2.20-2.35$, $D_r=26-32\%$), medium dense ($e=1.97-2.00$, $D_r=50-54\%$), and dense ($e=1.63-1.68$, $D_r=79-85\%$) states. These descriptions are consistent with those used in general geotechnical engineering practice (e.g., AS1726 – 1993). Effective confining pressures ranging from 50 kPa to 1600 kPa were applied.

The results of a series of undrained triaxial compression tests on loose samples of Pumice A sand with a relative density of 26-32% are presented in Figure 2 for an effective confining pressure range of up to 400 kPa. It can be seen that the test results showed strain hardening response at this range of pressure, with the deviator stress q increasing with increase in axial strain. Moreover, q increases with the confining pressure and at large strain level, the plots are more or less parallel to each other. From the stress paths, the specimen under lower confining pressure was less contractive than those under higher confining pressure. The stress-strain relations show a stiffer response at small strain level, followed by development of large strains and greater dilatancy when the phase transformation state (from contractive to dilative) is reached. Compared to natural sands where the stress-strain curves appear to merge at large strain range (i.e., steady state of deformation), the curves for pumice sand do not converge, at least within the strain level shown, possibly limited by the capability of the testing apparatus.

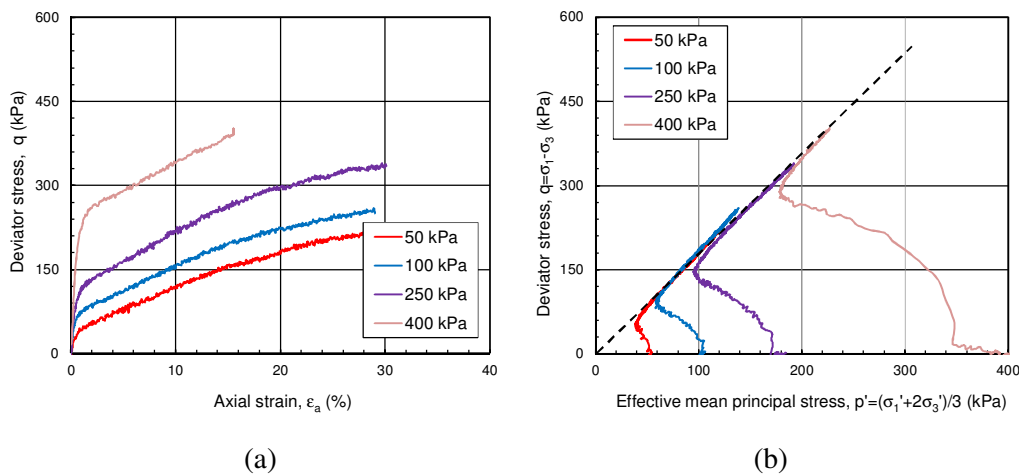


Figure 2. Test results for loose Pumice A sands: (a) stress-strain relation; and (b) effective stress paths.

The results for two other series of tests, this time on medium dense ($D_r=50-54\%$) and dense ($D_r=79-85\%$) states are presented in Figures 3 and 4, respectively. Considering the influence of initial confining pressure on the stress-strain relation and pore water pressure response, similar tendencies are observed in the overall behaviour of dense and loose pumice specimens. This

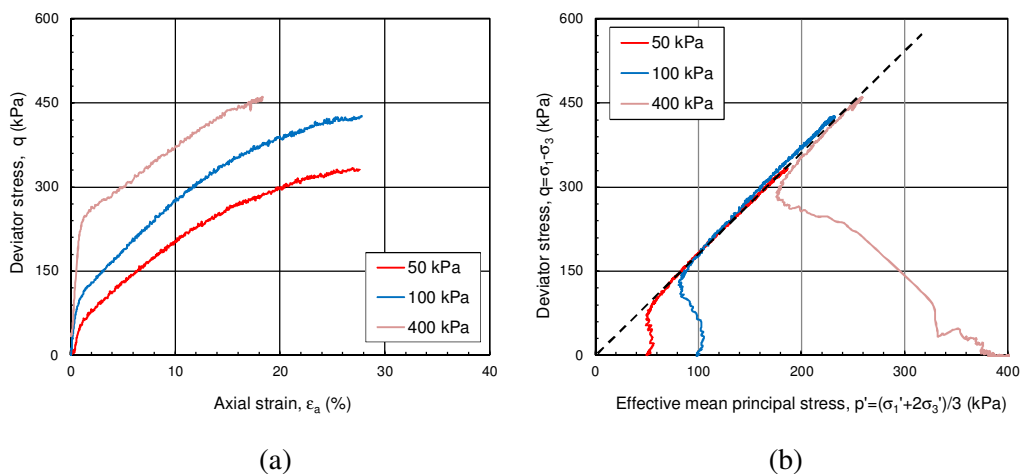


Figure 3. Test results for medium-dense Pumice A sands: (a) stress-strain relation; and (b) effective stress paths.

observation indicates that relative density is not a good parameter to differentiate the response of pumice sands, consistent with the observation made by Wesley et al. 1999. Moreover, all the tests showed similar tendency of stiff response at small strain level, followed by large straining when the phase transformation state is reached.

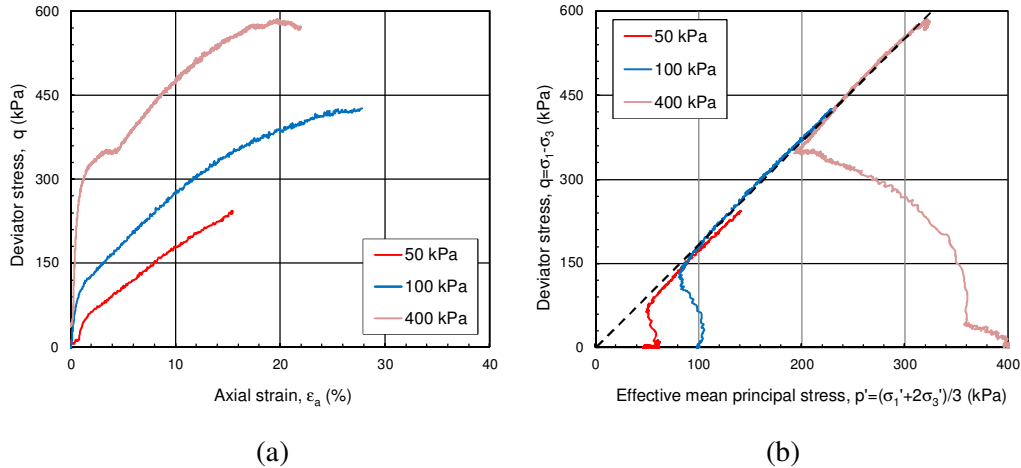


Figure 4. Test results for dense Pumice A sands: (a) stress-strain relation; and (b) effective stress paths.

Tests were conducted at very high confining pressure; however, problems were encountered in some cases because of the limitation of the apparatus. Nevertheless, a clear trend was observed in the tests which were successful. Figure 5 shows the monotonic undrained test results for dense Pumice B sands subjected to $\sigma_c' = 400, 800$ and 1600 kPa. Whereas the results for 400 kPa showed strain hardening behaviour, those at higher pressures manifested strain softening response, especially at large strain level. This behaviour is similar to those observed in Toyoura sand (Ishihara 1996). However, it can be seen from the figure that even at strain levels as large as 40% , the stress-strain curves did not converge to the steady state. Also noticeable is the stiff response of pumice at small strain range, followed by large deformation after the phase transformation was reached.

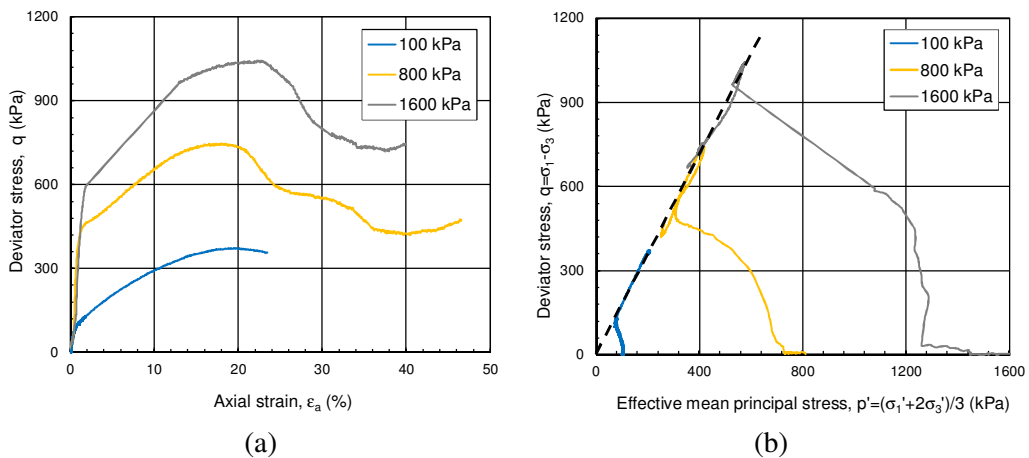


Figure 5. Test results for dense Pumice B sands: (a) stress-strain relation; and (b) effective stress paths.

3.2 Effect of soil gradation

Next, the monotonic undrained response of Pumice A and Pumice B sand specimens are compared. Figure 6 shows the comparison of results for the two specimens at $\sigma'_c=100$ kPa and 400 kPa. It can be observed that while the stress-strain curves are more or less similar, the development of excess pore water pressure appears to be faster for Pumice B sands. Similar general tendencies were also observed in the other test comparisons. Thus, the finer-grained Pumice B sand appears to be more liquefiable when compared to Pumice A sand.

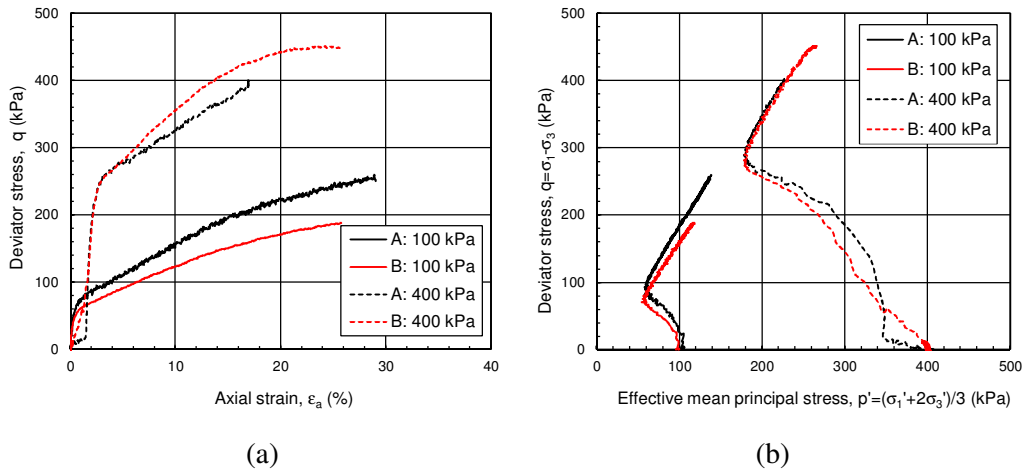


Figure 6. Test results for dense Pumice B sands: (a) stress-strain relation; and (b) effective stress paths

For the cases shown in Figures 2-4, it can be observed that for the specimen of particular density, the effective stress paths become asymptotic to the failure line, indicated by the dashed lines in the figures. The slope of the line, M_f , can be correlated to the angle of inter-particle friction ϕ_f using the following equation:

$$M_f = \left(\frac{q}{p'} \right) = \frac{6 \sin \phi_f}{3 - \sin \phi_f} \quad (1)$$

For all the densities considered, the values of the inter-particle friction angle were calculated for both Pumice A and B sands and the results are summarised in Table 1. Regardless of the density, the angle ϕ_f for each type of pumice sand appears to be constant, with values of 42° and 44° for pumice B and A, respectively. Thus, pumice A has higher ϕ_f and therefore a little bit higher shear resistance than pumice B.

Table 1. Values of inter-particle friction angle at failure, ϕ_f , for pumice

	Pumice A sand	Pumice B sand
Loose	44	42
Medium dense	44	42
Dense	44	42

For comparison purposes, typical values for loose natural sands are in the order of $\phi_f=30^\circ$. The higher frictional angle of pumice may be attributed to their crushable nature as well as the particle's very angular shape.

Using the same concept, the locus of points in the p' - q plane representing the phase transformation state (from contractive to dilative behaviour) can be obtained for each test

condition. Results indicate that the angle at phase transformation, ϕ_{pt} , ranges from 34-36° for Pumice B and 36-37° for pumice A sand. Again, these values are much larger than those typically observed for natural sands.

3.3 Investigation of Particle Crushing

To investigate whether particle breakage occurred during monotonic shearing, sieve analyses were conducted after most of the tests. A comparison of the grain size distribution before and after the undrained shear test for dense Pumice B sand at $\sigma'_c=400$ kPa is shown in Figure 7. For the level of shearing the specimen was subjected to, considerable particle crushing occurred.

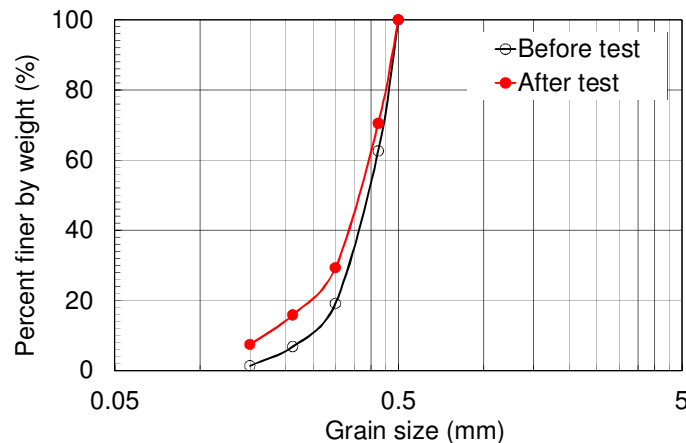


Figure 7. Grain size distribution curves of dense Pumice B specimen before and after test ($\sigma'_c=400$ kPa).

As pointed out by Kikkawa et al. (2012), pumice particles are very fragile not only because they are porous but also because they are angular in shape; it is the combination of these two factors that makes the particles highly crushable. It is postulated that the axial strain measured during the test is the result of both load-induced compression of the specimen and particle crushing; as a result, the structure of pumice specimen becomes more stable with continuous shearing, accounting for the predominantly strain-hardening response observed in the tests. In addition, the changing particle size distribution during the course of undrained test makes the pumice soil more resistant to deformation when compared to specimens consisting of hard-grained sands.

3.4 Steady state concept

Numerous studies on the undrained monotonic behaviour of sand have used the steady state concept to discuss the response. The steady state of deformation, also known as critical state, is defined as the state at which a sandy soil deforms under constant shear stress, constant effective stress and constant volume (Casagrande, 1976; Castro and Poulos, 1977). The strength and mean effective stresses which occur at the steady state of deformation change as the density of sand is varied, enabling a 'steady state line' to be defined in $e - q - p'$ space. The projection of this line in the $e - p'$ plane is often presented to discuss the response of sand at the steady state of deformation. Initial states with densities lower than those of the steady state line tend to result in contractive soil response during monotonic loading, whilst initial states with densities higher than the steady state line tend to dilate during loading. Note however that the steady state line only provides an approximation for division between initial states that contract or dilate (Cubrinovski and Ishihara, 2000) – the initial dividing line (Ishihara, 1993) actually marks the boundary between contractive and dilative initial states.

Looking at the earlier test results, it is seen that the steady state condition was not reached in the tests. The deviator stress continues to increase even when large deformation was reached ($\epsilon_a > 25\%$). The breakage of the particles does not allow for the pumice sand to deform under constant shear stress, constant effective stress and constant volume. In fact, at large deformation, the specimens tend to deform irregularly, as shown by typical deformation modes illustrated in Figure 8. Thus, meaningful data at the end of the tests were not obtained.

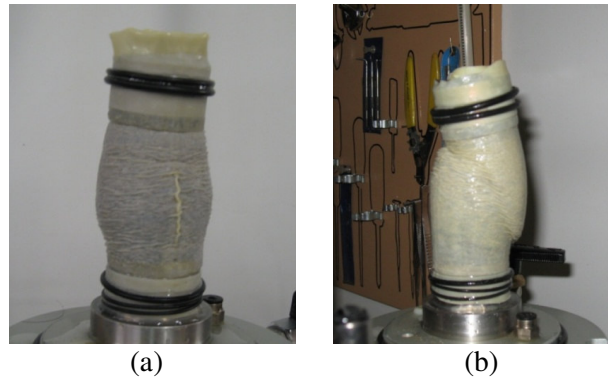


Figure 8. Deformed shape of Pumice B specimens after monotonic undrained tests: (a) $\sigma'_c=100$ kPa; (b) $\sigma'_c=400$ kPa.

Although limited in scope, the monotonic undrained tests on pumiceous specimens presented herein showed that the steady state was not reached in the tests. Because the particles are crushed as the deviator stress is applied, the soil structure becomes more stable and resistance increases; as a result the condition of constant deformation under constant shear stress (and constant volume) was not achieved, at least within the strain range allowed by the triaxial apparatus used. It follows that the framework of critical soil mechanics may not be applicable to crushable sands like pumice. More experiments are recommended to confirm this.

4 CONCLUDING REMARKS

Under monotonic undrained loading, pumice specimens reconstituted under loose and dense states practically showed similar response, indicating that relative density did not have significant effect on its behaviour. Within the range of effective confining pressures investigated, pumice specimens showed contractive response followed by dilative behaviour. The contractive response was more significant at high confining pressure. The stress-strain relations showed a stiffer response at small strain level, followed by development of large strains and greater dilatancy when the phase transformation state is reached.

Pumice sands have angles of internal friction of about $42-44^\circ$, and these values were not affected by relative density. It was noted that these were far greater than those for natural hard-grained sands. The friction angles at phase transformation were between $34-37^\circ$, which were again much higher than those of natural sands. Even under large strain level, pumice sands did not reach steady state of deformation. This can be attributed to breakage of particles during shearing, which resulted in more resistant soil structure that did not allow deformation at constant shear stress to occur.

ACKNOWLEDGMENTS

The author would like to acknowledge the assistance of Messrs Y Lu, C Chan and N Taghipouran in performing the laboratory tests presented herein. This research was made possible through the Earthquake Commission (EQC) Biennial Contestable Grant No. 10/589.

REFERENCES

- Casagrande, A. (1976). Liquefaction and cyclic deformation of sands: A critical review. *Harvard Soil Mechanics Series*, 88.
- Castro, G. & Poulos, S. J. (1977). Factors affecting liquefaction and cyclic mobility. *J Geotech Eng Div, ASCE*, 103, 501 – 516.
- Cubrinovski, M. & Ishihara, K. (2000). Flow potential of sandy soils with different grain compositions. *Soils and Foundations*, 40, 103 – 119.
- Ishihara, K. (1993). Liquefaction and flow failure during earthquakes. *Geotechnique*, 43, 351 – 415.
- Ishihara, K. (1996). *Soil Behaviour in Earthquake Geotechnics*, Oxford Science.
- Kikkawa, N. (2008). Stress relaxation during Ko compression of pumice sand. *Proc. 8th ANZ Young Geotechnical Professionals Conference 2008*, Wellington, 97 – 102.
- Kikkawa, N., Pender, M.J., Orense, R.P. & Matsushita, E. (2009). Behaviour of pumice sand during hydrostatic and Ko compression. *Proceedings, 17th International Conference on Soil Mechanics and Geotechnical Engineering*, Alexandria (Egypt), Vol. 1, 812 – 815.
- Kikkawa, N., Orense, R.P. & Pender, M.J. (2011). Mechanical behaviour of loose and heavily compacted pumice sand. *Proc., 14th Asian Regional Conference on Soil Mechanics and Geotechnical Engineering*, Hong Kong, Paper 214. 6pp.
- Kikkawa, N., Orense, R.P. & Pender, M.J. (2012). Observations on microstructure of pumice particles using computed tomography. *Canadian Geotechnical Journal* (submitted).
- New Zealand Standard (1986). *NZS 4402: 1986 - Methods of Testing Soils for Civil Engineering Purposes*. Part 2 Soil classification tests. 2.7 Determination of the solid density of soil particles. Test 2.7.2 Method for medium and fine soils.
- Orense, R.P., Pender, M.J. & Tai, A. (2012). Undrained cyclic shear behaviour of pumice sand, *11th Australia New Zealand Conference on Geomechanics (ANZ 2012)*. Melbourne, 858 – 863.
- Pender, M. J. (2006). Stress relaxation and particle crushing effects during Ko compression of pumice sand. *Proc. International Symposium on Geomechanics and Geotechnics of Particulate Media*, Yamaguchi, Japan, Vol.1, 91 – 96.
- Pender, M.J., Wesley, L.D., Larkin, T.J. & Pranjoto, S. (2006). Geotechnical properties of a pumice sand. *Soils and Foundations*, 46, (1), 69 – 81.
- Wesley, L. D., Meyer, V. M., Pranjoto, S., Pender, M. J., Larkin, T. J. & Duske, G. C. (1999). Engineering properties of pumice sand. *Proc. 8th Australia-NZ Conference on Geomechanics*, Hobart, Vol. 2, 901 – 908.